PELDOR at S- and X-Band Frequencies and the Separation of Exchange Coupling from Dipolar Coupling

Axel Weber, Olav Schiemann,[1] Bela Bode, and Thomas F. Prisner

Institut für Physikalische und Theoretische Chemie, Johann Wolfgang Goethe-Universität, Marie-Curie-Strasse 11, 60439 Frankfurt/Main, Germany

A pulsed electron double resonance (PELDOR) setup working at S-band frequencies is introduced and its performance compared with an X-band setup. Furthermore, to verify experimentally that it is possible to disentangle the dipolar coupling ν_{Dip} from the exchange coupling J by PELDOR we synthesized and investigated four bisnitroxide radicals. They exhibit in pairs the same distances r_{AB} between the nitroxide moieties but only one of each pair possesses a non-zero J. The experimental values for r_{AB} match the ones from molecular modeling very well for the molecules without exchange coupling. For one bisnitroxide it was possible to separate ν_{Dip} from J and to ascertain the magnitude and sign of J to $+11$ MHz (antiferromagnetic spin–spin coupling).   © 2002 Elsevier Science (USA)

Key Words: dipolar coupling; PELDOR; S-band EPR; pulse EPR; exchange coupling.

INTRODUCTION

There is a strong interest in structures and dynamics of organic polymers (*1*) and biomolecules like proteins (*2*) or RNA (*3*) driven by the paradigm that the structure determines its properties or function. Commonly used methods to gain insight into the structure of these molecules are X-ray crystallography (*4*), fluorescence energy transfer (FRET) measurements (*5*), as well as nuclear magnetic resonance (NMR) (*6*), and electron paramagnetic resonance (EPR) spectroscopy (*7*). X-ray crystallography can provide precise global and local structure information. But it is restricted to studies of molecules in crystals, where, for example, an enzyme may not be in the catalytically active form. Complementary to that, NMR, FRET, and EPR are methods capable of collecting structural data from these molecules in solution. However, to be able to apply EPR spectroscopic tools the molecule needs to possess paramagnetic centers. If it does not site-directed spin-labeling by nitroxides is a commonly used way to overcome this problem (*8*). Twofold spin-labeling makes it then possible to gather structural information about the labeled molecule by measuring the coupling energy $E_{\mathrm{AB}} = h\nu_{\mathrm{AB}}$ between the two unpaired electrons with spins S_{A} and S_{B} (*9*). E_{AB} is the eigenvalue of the electron–electron coupling

Hamiltonian H_{AB} [1], which is defined as the sum of the Hamiltonian H_{D} [2] for the magnetic dipole–dipole coupling and the Hamiltonian H_J [3] for the exchange coupling.

$$H_{\mathrm{AB}} = H_{\mathrm{D}} + H_J \qquad [1]$$

with

$$H_{\mathrm{D}} = S_{\mathrm{A}} D S_{\mathrm{B}} \qquad [2]$$

and

$$H_J = J S_{\mathrm{A}} S_{\mathrm{B}}. \qquad [3]$$

Here D is the magnetic dipole–dipole coupling tensor and J is the electron–electron exchange coupling constant. In first-order high-field approximation the electron–electron coupling ν_{AB} can be expressed by Eqs. [4] and [5] as the sum of the orientation-dependent magnetic dipole–dipole coupling constant ν_{Dip} and the isotropic exchange coupling constant J.

$$\nu_{\mathrm{AB}} = \nu_{\mathrm{Dip}}(3\cos^2\theta - 1) + J \qquad [4]$$

with

$$\nu_{\mathrm{Dip}} = \frac{\mu_{\mathrm{B}}^2 g_{\mathrm{A}} g_{\mathrm{B}} \mu_0}{4\pi h} \frac{1}{r_{\mathrm{AB}}^3}. \qquad [5]$$

θ is the angle between the applied magnetic field B_0 and the interspin distance vector $\mathbf{r}_{\mathrm{AB}}$, μ_{B} is the Bohr magneton, μ_0 is the field constant and g_{A}, g_{B} are the g values of the unpaired electrons A and B, respectively. The orientation dependence of ν_{AB} is depicted in Fig. 1. From ν_{Dip} the spin–spin distance r_{AB} can be calculated and it may, for example, be rationalized if a molecule is stretched or bent or if its structure changes upon binding to another molecule.

With continuous wave (cw) EPR spectroscopy distance measurements are limited due to the spectral linewidth of the nitroxides to a maximum distance of about 20 Å (*10*). However, since the linewidth of the nitroxides is determined by unresolved hyperfine splittings and inhomogeneous line broadening, pulsed

---

[1] To whom correspondence should be addressed. Fax: 069-798-29404. E-mail: olav@prisner.de.
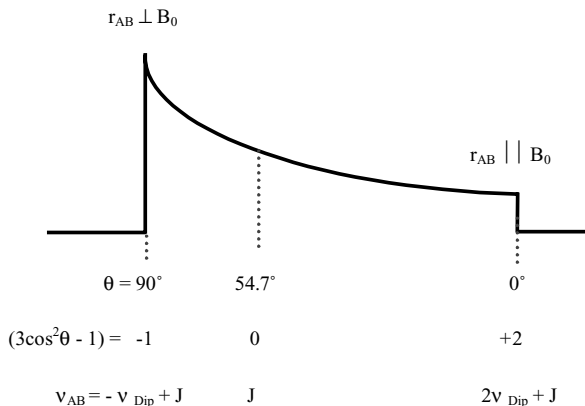
FIG. 1. The powder pattern for ν_{AB} with the singularities and the related θ angles.

EPR spectroscopy is a way to raise this limit by designing pulse sequences which recover the spin–spin coupling and suppress other spectral contributions. In 1981 Milov *et al.* established the pulsed electron double resonance (PELDOR) method (*11*) with the well-known three-pulse pattern. Here a $\pi/2 - \tau - \pi$ detection
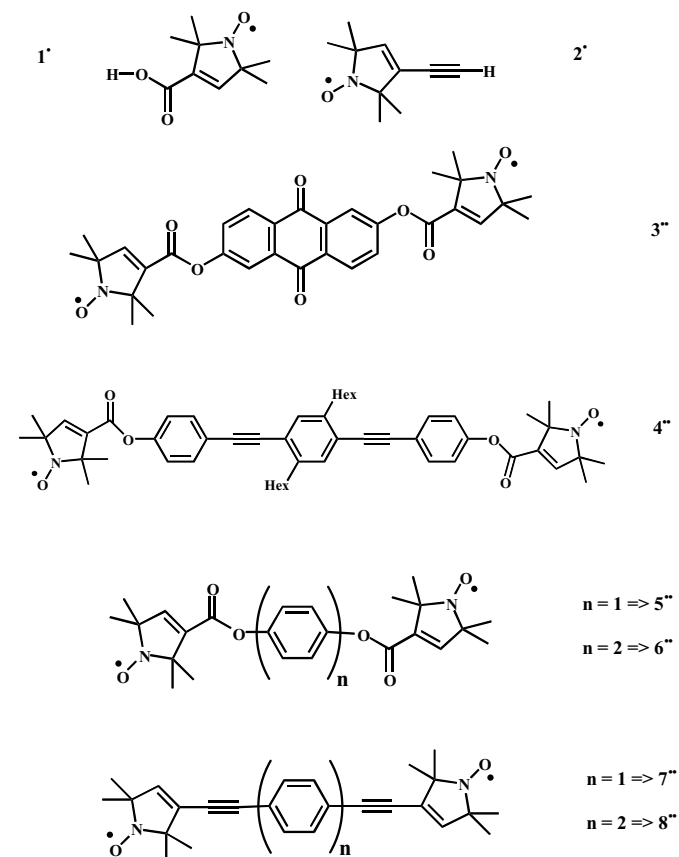
FIG. 2. Structures of the inquired radicals $1^\bullet$ to $8^{\bullet\bullet}$ in the stretched conformation as used for molecular modeling (Hex, *n*-hexyl groups).

sequence at microwave frequency ν_1 excites spin A in a biradical and creates a Hahn echo. Spin B in the same molecule is excited by an additional inversion pulse at microwave frequency ν_2 whereupon the amplitude Φ of the Hahn echo shows an oscillation dependent on the position T of the inversion pulse. The frequency of this oscillation is the coupling ν_{AB}. Jeschke and co-workers extended PELDOR to a dead time free four-pulse sequence (*12*) and derived a single frequency technique for refocusing dipolar couplings (SIFTER) (*13*) from the solid-echo well known in NMR (*14*). Two other pulse experiments capable of measuring ν_{AB} are "2 + 1" from Kurshev *et al.* (*15*) and "DQC" from Saxena and Freed (*16*).

In the paper presented here the technical setup for PELDOR measurements at S-band frequencies, its successful testing, and its performance with respect to an X-band PELDOR setup are described. The advantage of carrying out PELDOR experiments at two different frequencies is to be able to separate the wanted ν_{AB} coupling from residual hyperfine coupling contributions (*17*). In all previous publications PELDOR measurements were performed at X-band frequencies. However, Raitsimring and co-workers announced S- and C-band PELDOR measurements in two conference contributions (*18*). Furthermore we show that in the case of exchange-coupled biradicals it is possible to determine experimentally not only ν_{Dip} but also the magnitude and sign of *J*. This is achieved by detecting with PELDOR both tensor singularities of ν_{AB} (Fig. 1) and using (*19*)

$$\nu_{Dip} = (\nu(\theta_\parallel) - \nu(\theta_\perp))/3 \qquad [6]$$

$$J = (2\nu(\theta_\perp) + \nu(\theta_\parallel))/3. \qquad [7]$$

In this way it is possible to calculate the spin–spin distance r_{AB} even in the case of an exchange-coupled biradical. As examples the bisnitroxides $5^{\bullet\bullet} - 8^{\bullet\bullet}$ were synthesized (Fig. 2), where the conjugated bridges in $7^{\bullet\bullet}$ and $8^{\bullet\bullet}$ facilitate an exchange coupling through bonds whereas the ester linkages in $5^{\bullet\bullet}$ and $6^{\bullet\bullet}$ disrupt this conjugation and therefore diminish the exchange coupling while leaving the r_{AB} almost unchanged.

SYNTHESIS AND SAMPLE PREPARATION

Radical $2^\bullet$ (2,2,5,5-tetramethyl-3-pyrroline-1-oxyl-3-acetylene) was prepared from 2,2,5,5-tetramethyl-3-pyrroline-1-oxyl-3-carboxylic acid $1^\bullet$ with slight modifications to the procedure described by Hideg *et al.* (*20*). Biradicals $3^{\bullet\bullet}$ and $4^{\bullet\bullet}$ were donated to us by G. Jeschke and used as received. The new biradicals $5^{\bullet\bullet} - 6^{\bullet\bullet}$ were synthesized in analogy to (*21*).

Biradical $5^{\bullet\bullet}$. To a solution of 46 mg (0.42 mmol) 1,4-dihydroxybenzene, 230 mg (1.25 mmol) 2,2,5,5-tetramethyl-3-pyrroline-1-oxyl-3-carboxylic acid $1^\bullet$, and 171 mg (1.4 mmol) dimethylaminopyridine in 5 ml dry THF were added 1.25 ml of a 1 M solution of *N,N*-dicyclohexylcarbodiimide in methylenechloride (1.25 mmol) at 0°C. The yellow reaction mixture was stirred at room temperature for 20 h. The precipitate was

filtered off and washed with THF until the solid was color-less. The yellow filtrate was washed with 2 N HCl and brine. The organic phase was dried with $MgSO_4$ and concentrated *in vacuo*. The remaining yellow solid was redissolved in warm dichloromethylene and applied onto a silica gel column. Using diethyl ether : pentane (1 : 1) as the eluent yielded $5^{\bullet\bullet}$ in the second band ($R_f = 0.35$). An additional HPLC purification (CH_2Cl_2 : hexane : ethyl acetate = 7 : 5 : 2) provided pure $5^{\bullet\bullet}$ as yellow powder with a yield of 25 mg (11%). MALDI-MS (ATT-Matrix): $m/z = 444.2$ (100% $M^+ + 2H$), 442.2 (100% M+), 428.6 (60% –CH_3). FT-IR (KBr): 3080(m), 2980(m), 2930(m), 1730(s), 1625(m), 1505(s), 1175(s), 790(m) cm^{-1}. Elemental analysis calculated for $C_{24}H_{30}N_2O_6$ (442.5): C 65.14, H 6.83, N 6.33; found C 64.92, H 7.00, N 5.91.

Biradical $6^{\bullet\bullet}$.   To a solution of 78 mg (0.42 mmol) 4,4′-dihydroxybiphenyl, 230 mg (1.25 mmol) 2,2,5,5-tetramethyl-3-pyrroline-1-oxyl-3-carboxylic acid $1^{\bullet}$, and 171 mg (1.4 mmol) dimethylaminopyridine in 5 ml dry THF were added 1.25 ml of a 1 M solution of N,N-dicyclohexylcarbodiimide in methyl-enechloride (1.25 mmol) at 0°C. The reaction mixture was stirred at room temperature for 20 h, and the precipitate filtered off and washed with THF until the solid was colorless. The yellow fil-trate was washed with 0.5 N HCl and brine. The organic phase was dried with $MgSO_4$ and concentrated *in vacuo*. The solid was redissolved in warm dichloromethylene and applied onto a silica gel column. Using diethyl ether : pentane (1 : 1) as the elu-ent yielded $6^{\bullet\bullet}$ in the second band ($R_f = 0.3$). An additional HPLC purification (CH_2Cl_2 : hexane : ethyl acetate = 7 : 5 : 2) gave pure $6^{\bullet\bullet}$ as a yellow powder with a yield of 30 mg (16%). MALDI-MS (ATT-Matrix): $m/z = 520.4$ (95% $M^+ + 2H$), 518.5 (100% M+), 504.3 (50% -CH_3). FT-IR (KBr): 3065(m), 2980(m), 2935(m), 1735(s), 1625(m), 1490(s), 1195(s), 795(m) cm^{-1}. Elemental analysis calculated for $C_{30}H_{34}N_2O_6$ (518.61): C 69.48, H 6.61, N 5.40; found C 68.95, H 6.89, N 4.78.

Biradical $7^{\bullet\bullet}$.   Biradical $7^{\bullet\bullet}$ was synthesized from $2^{\bullet}$ as follows. A solution of 100 mg (0.6 mmol) of $2^{\bullet}$ and 99 mg (0.3 mmol) of 1,4-diiodbenzene in 5 ml of N,N-dimethylformamide was deoxygenated by repeated exposure to vacuum, followed by the addition of nitrogen. The amounts of 132 mg (0.114 mmol) tetrakis(triphenylphosphine)palladium(0) and 290 mg (1.53 mmol) copper(I)iodide were added, and the solution was deoxygenated once more. The amount of 73 mg (0.72 mmol) triethylamine was added via a syringe, and the re-sulting mixture was stirred at 25°C for 12 h. The volatiles were removed *in vacuo* and the residue was dissolved in toluene. Chromatography on silica gel (Toluol : THF = 17 : 1) followed by HPLC (hexane : CH_2Cl_2 : ethyl acetate = 5 : 2 : 1) purification of the product fraction yielded $7^{\bullet\bullet}$ as a pale yellow powder (yield: 30 mg, 10%). EI-MS: $m/z = 403.1$ (79,5% M+), 388.2 (13% –CH_3), 373.5 (15% –CH_3), 358.2 (100% –CH_3), 342.0 (12% –CH_3). FT-IR (KBr): 3050(m), 2980(s), 2930(m), 2220(w), 835(m) cm^{-1}. Elemental analysis calculated for $C_{26}H_{30}N_2O_2$ (402.54): C 77.58, H 7.51, N 6.96; found C 77.38, H 7.61, N 6.74.

Biradical $8^{\bullet\bullet}$.   Biradical $8^{\bullet\bullet}$ was synthesized and purified according to the procedure described for $7^{\bullet\bullet}$ but with the use of 4,4′-diiodbiphenyl instead of 1,4-diiodbenzene (yield 20 mg, 7%). EI-MS: $m/z = 478.6$ (20,3% M+), 463.6 (6% –CH_3), 448.5 (22% –CH_3), 433.6 (8% –CH_3), 418.5 (100% –CH_3). FT-IR (KBr): 3050(m), 2980(s), 2930(m), 2215(w), 825(m) cm^{-1}. Ele-mental analysis calculated for $C_{32}H_{34}N_2O_2$ (478.64): C 80.30, H 7.16, N 5.85; found C 80.40, H 7.10, N 5.92.

For the EPR measurements appropriate amounts of biradicals $3^{\bullet\bullet}$–$8^{\bullet\bullet}$ were dissolved in h_8- or d_8-toluene to yield 160 μl of 1 mM solutions. The pulsed S-band measurements were carried out at 10 K and the respective X-band measurements at 20 K.

EPR INSTRUMENTATION AND DEVELOPMENTS

X-band.   The cw X-band EPR spectra were recorded on a Bruker ESP300e EPR spectrometer. The pulsed X-band exper-iments were carried out on an ELEXSYS E580 pulsed X-band EPR spectrometer from Bruker with the technical specifications as described in (*22*). For the PELDOR experiments this spec-trometer was extended in such a way that a second microwave frequency could be fed into the microwave pulse forming unit (MPFU) within the bridge. The second microwave frequency was generated by a HP 8672A synthesizer and amplified by a Miteq AMF-5B-080120-30-25P amplifier to achieve the desired power of +17 dBm. Following the amplifier a directional coupler Narda 3004-10 fed −10 dB for power measurements into a spec-trum analyzer 492 from Tektronix. The signal from the other exit was coupled into one of the two MPFUs in the ELEXSYS E580 microwave bridge. A phase-insensitive detection of the power level of both pulse frequencies was accomplished by placing a Narda 3004-10 directional coupler before the TWT and feeding −10 dB into a MDC 1118-S diode from Midisco. The signal from this diode was viewed by a LeCroy 9350AM oscilloscope. In all X-band experiments a commercial flex line probehead with a dielectric ring resonator from Bruker was used which exhibits in overcoupled conditions a resonance frequency ν_0 of 9.7 GHz, a quality factor Q of about 100, a conversion factor κ of 4 $\mu T/\sqrt{W}$ and a bandwidth of 97 MHz. Accordingly, even with a frequency offset of 80 MHz between ν_0 and ν_2 both pulses are still within the bandwidth of the resonator.

S-band.   The S-band EPR experiments were performed on a home-built cw/pulsed S-band EPR spectrometer (*23*). As the second source a synthesizer 4002 from Schlumberger was used. Since it generates only microwave frequencies up to 2.16 GHz a frequency doubler MX2J020040 from Miteq was necessary to convert the frequency up to S-band. A variable microwave power attenuator Narda 791FM following the frequency doubler makes it possible to adjust the power of the microwave signal. From there the microwave propagates through an isolator FG1-1 L1FFL1 and reaches a PIN switch HP 33144A. If the PIN switch is closed the microwave is reflected and absorbed by the isolator, if the switch is open the microwave is combined with the signal of the first source at a two-way power combiner ANAREN 41130.
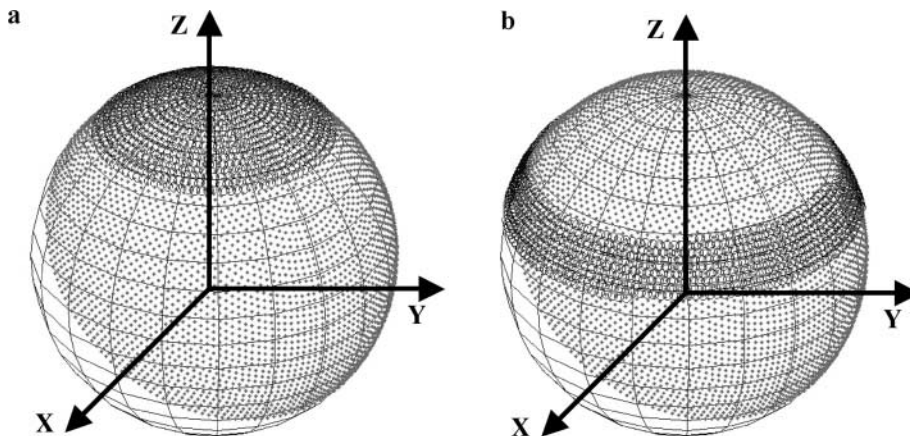
FIG. 3. Computed orientation selection in the hyperfine axis system for the pump (points) and the detection pulses (open circles) at (a) $\Delta \nu = 80$ MHz and (b) $\Delta \nu = 40$ MHz. The calculations were done with rectangular pulses of 25 MHz width and for only one hemisphere.

Both microwaves are then guided through an isolator M312040 to a fast PIN switch S136ADU1 from Miteq (switching time <2 ns). A GaAs-amplifier AMA2040B (gain 45 dB) amplifies the pulses to +30 dBm in order to provide an optimal power level for the subsequent Litton 624 pulsed 1 kW traveling wave tube (TWT) amplifier. A 10 dB directional coupler Narda 3003-10 placed before the TWT amplifier serves in conjunction with a detector diode MDC1118-S from Midisco as a transmitter monitor, which is necessary to compare the amplitude of the pulses of the second frequency with the amplitude of the pulses of the first one.

All S-band experiments were performed with a home-built bridged loop gap resonator exhibiting in overcoupled conditions a resonance frequency ν_0 of 3.60 GHz, a quality factor Q of 150 and a bandwidth of 24 MHz. Therefore even with the smallest frequency offset $\Delta \nu = \nu_1 - \nu_2$ of 40 MHz used in our experiments it is not possible to have both frequencies ν_1 and ν_2 within the bandwidth of the resonator. Nevertheless, due to the large conversion factor κ of 15 $\mu T/\sqrt{W}$ it is possible to achieve a flip angle of 180° for typical pulses of 40 ns duration, up to a frequency offset of 100 MHz from the center ν_0 of the resonator. To ensure a flip angle of 180° for the inversion pulse at the off-resonant frequency ν_2 a Hahn echo was created at this frequency and the power optimized.

The sensitivity of the pulsed S-band spectrometer was measured to be three times smaller then at X-band and in agreement with theory (*24, 25*).

ORIENTATION SELECTIVITY

The PELDOR measurements were performed with pulse lengths of 40 ns at S-band and of 32 ns at X-band for all three pulses. Since the corresponding spectral widths of the pulses of 25 and 35 MHz for S- and X-band, respectively, are smaller than the nitroxide field swept spectra (~200 MHz) the pulses are selecting certain molecular orientations. Which orientations are selected depends on the position of the pulses with respect to the field swept spectrum. In all experiments the inversion pulse was exciting the ^{14}N $m_I = 0$ hyperfine line resulting in the excitation of only a fraction of the nitroxide moieties but of all orientations with respect to B_0. From these molecules those are contributing to the PELDOR modulation for which the second nitroxide group is selected by the detection sequence. If the detection sequence has a frequency offset $\Delta \nu$ of 80 MHz from the inversion pulse the field swept spectra of the nitroxides under study consist mostly of the $m_I = +1$ component of the $A_{ZZ}(^{14}N)$ hyperfine coupling leading to a selection of 1/3 of those molecules with the second nitroxide oriented with A_{ZZ} parallel to B_0 (Fig. 3a). If $\Delta \nu$ equals 40 MHz the selection profile of the detection pulses is shifted closer to equatorial orientations of the hyperfine tensor (Fig. 3b). This hyperfine orientation selectivity results for both $\Delta \nu$'s in a θ selection depending on the orientation of $\mathbf{r}_{AB}$ with respect to the hyperfine tensor. However, additional orientations to those displayed in Fig. 3 are excited by the whole profile of the pulses but to a lesser extent. This may lead to the detection of both dipolar tensor singularities with one measurement especially if the weak $\theta_{\parallel} = 0°$ dipolar tensor singularity is excited within the bandwidth of the detection pulses whereas the intense $\theta_{\perp} = 90°$ is excited by the side loops only. The θ values can then be assigned by comparing the measurements at $\Delta \nu = 80$ and 40 MHz and ν_{Dip} and J can be calculated according to Eqs. [6] and [7].

MEASUREMENTS AND DISCUSSION

The S- and X-band PELDOR setups described above were tested on the bisnitroxides $3^{\bullet\bullet}$ (*26*) and $4^{\bullet\bullet}$ (*12a*) known from literature. With a $\Delta \nu$ of 80 MHz $3^{\bullet\bullet}$ and $4^{\bullet\bullet}$ displayed in both frequency bands an oscillation frequency ν_{AB} of 6.8 and 2.1 MHz, respectively. These data match the X-band PELDOR data from the literature nicely (Table 1) and confirm that both PELDOR units are working properly. To calculate the spin–spin distance r_{AB} according to Eqs. [4] and [5] the θ value belonging to the

TABLE 1
Data for 5[••]–8[••] Gathered from S- and X-Band PELDOR Measurements

Molecule	$\nu_{AB}(\theta_\perp)$ (MHz)[a]	$\nu_{AB}(\theta_\parallel)$ (MHz)[a]	ν_{Dip} (MHz)	J^{PELDOR}/J^{CW} (MHz)	r_{AB} (Å)[exp.]	r_{AB}[b] (Å)[theor.]
3[••]	6.8/6.8	13.4/13.8	6.8(2)	—	19.7(3)	19.7(10)[c]
4[••]	2.1/2.1	4.3/4.3	2.1(2)	—	29.2(4)	29.2(10)[d]
5[••]	14.1/14.2	—/—	14.2(2)	—	15.4(3)	15.5(10)
6[••]	6.9/6.9	—/13.7	6.9(2)	—	19.7(3)	19.7(10)
7[••]	—	—	—	—/73(3)	—	16.4(3)
8[••]	—/7.2	—/18.3	3.7(2)	+11.0(3)/12(3)	24.0(4)	21.0(3)

[a] The first number is from the S-band the second one from the X-band measurement.

[b] For the molecular modeling the N–O groups were replaced by N–OH groups and the theoretical r_{AB} measured from the midpoint of one N–O bond to the other.

[c] Larsen and Singel find the same experimental r_{AB} of 19.7 Å (26).

[d] Jeschke and co-workers measured an r_{AB} of 28.3(5) Å (12a).

measured ν_{AB} as well as the magnitude and sign of J need to be known. Thus the measurements were repeated with a $\Delta\nu$ of 40 MHz where the simulations showed that different orientations are selected (Fig. 3). The spectra of **3[••]** with $\Delta\nu = 40$ MHz are shown as an example in Fig. 4. The Fourier-transformed PELDOR spectra display at S-/X-band one peak at 6.8/6.8 MHz assigned to $\theta_\perp$ and another weaker one at 13.4/13.8 MHz corresponding to $\theta_\parallel$. Since the frequency at $\theta_\parallel$ is two times the frequency at $\theta_\perp$ it can be concluded that both singularities of the dipolar tensor were excited (28). It also confirms that the $\theta_\perp$ singularity was detected with $\Delta\nu = 80$ MHz. Using Eqs. [6] and [7] a negligible J and a ν_{Dip} of 6.8 MHz were found. With this an r_{AB} of 19.7 Å was calculated from Eq. [4]. That the weak peak assigned to $\theta_\parallel$ is not an artifact caused by hyperfine interaction is proven by the occurrence of this peak at the same frequency in the S- and X-band. In principle hyperfine interactions can contribute to PELDOR spectra as the occurrence of the free deuterium oscillation in the spectrum of monoradical **2[•]** showed. **4[••]** and **6[••]** showed in principle the same PELDOR behavior; their data are collected in Table 1. The experimental r_{AB} match for all three molecules those r_{AB} obtained by molecular modeling where the molecules adopted a stretched conformation (Table 1). The stretched conformation is also in agreement with the finding that A_{ZZ} is perpendicular to r_{AB}.

The shorter time window τ for the S-band compared to the X-band PELDOR measurements is caused by several properties of the electron spin echo (ESE) spectroscopy at low frequencies/low magnetic fields: (a) the deeper S-band electron spin echo envelope modulation (ESEEM) (Fig. 5) due to weak hyperfine interactions (25, 29), (b) the longer period of the Lamor frequencies, and (c) the reduced sensitivity as noted above. Additionally a shorter T_2-relaxation time was found for this sample even at the lower temperature compared to the X-band. Therefore, it was only possible to choose a few τ values where the ESE amplitude exhibits a maximum and a reasonable signal-to-noise ratio. The use of h_8-toluene as the solvent reduced the S-band

ESEEM depth from 100 to 80% and shortened its period but at the same time also the T_2-relaxation time from 0.8 to 0.4 μs so that in the end no improvement could be achieved. The PELDOR modulation depth is comparable in S- and X-band.
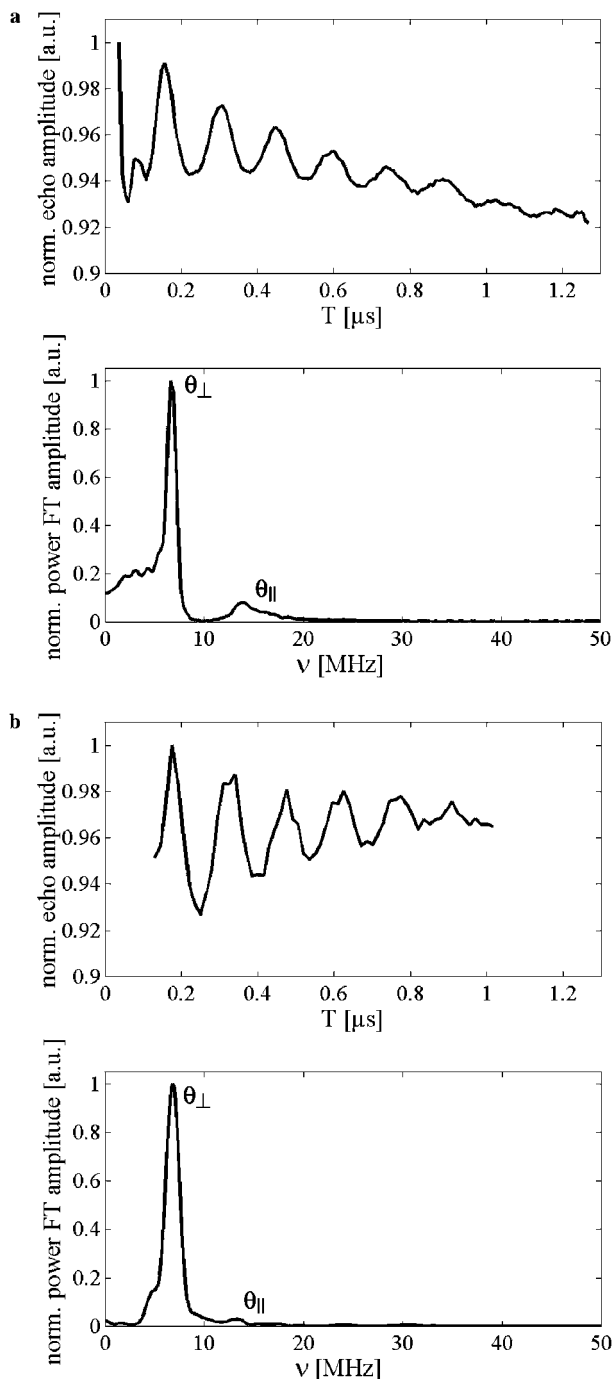
FIG. 4. Three-pulse PELDOR spectra of **3[••]** in d_8-toluene (a) at X-band with $\Delta\nu = 40$ MHz, the Fourier-transformed spectrum is shown below, and (b) at S-band with $\Delta\nu = 40$ MHz, the Fourier-transformed spectrum is shown below. Both time spectra were Fourier-transformed after subtracting the background caused by instantaneous diffusion (27).
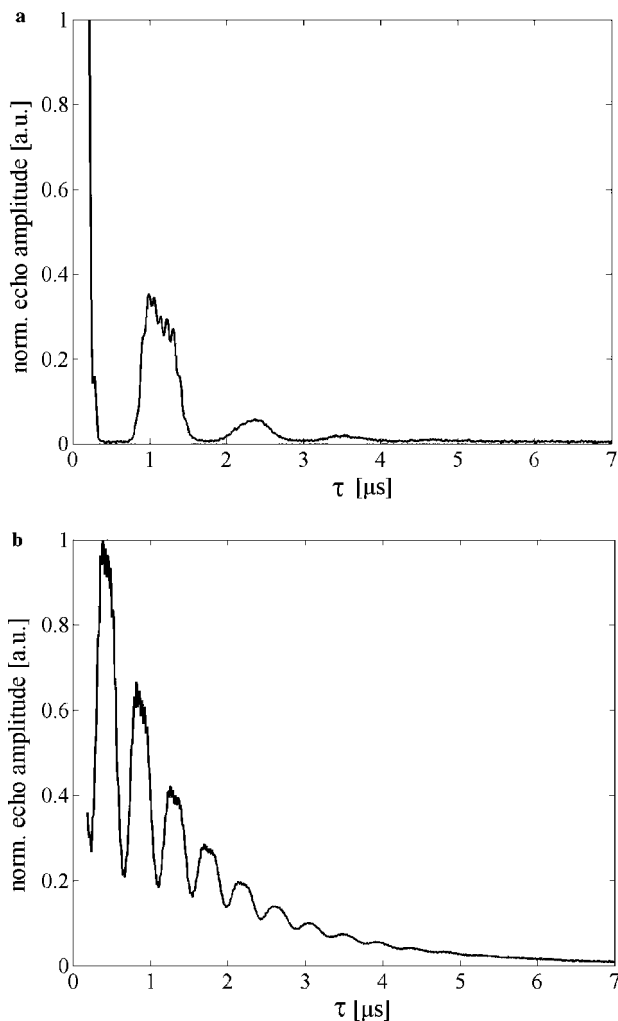
FIG. 5. Two-pulse ESEEM spectra of **3**•• in d_8-toluene at (a) S-band and (b) X-band.

For biradical **5**•• one peak was detectable at 14.2 MHz in X-band with $\Delta\nu = 80$ MHz (Fig. 6a), the second component of the tensor was not resolvable. However, since the nitroxide moiety and the field swept spectrum are the same as for **3**••, **4**••, and **6**•• it is reasonable to attribute this peak to $\theta_\perp$. Assuming secondly that J is negligible, because the two ester linkages prevent as in the case of **6**•• an exchange coupling, the measured ν_{AB} of 14.2 MHz can be assigned to ν_{Dip}. A spin–spin distance r_{AB} of 15.4 Å is calculated from that, matching nicely the distance obtained by molecular modeling and supporting thereby the assumptions. To ensure that the observed peak is not solely due to the free proton frequency we also performed S-band measurements (Fig. 6b), which revealed one peak at 14.1 MHz and one at 5.3 MHz. Since the peak at 14.2 MHz did not change its frequency upon changing the magnetic field from 3435 to 1249 G, this proves that it is due to dipolar electron–electron coupling. Nevertheless, the second peak in the S-band spectrum at 5.3 MHz corresponds to the free proton frequency, showing

the importance of being able to perform PELDOR at two different principal frequencies.

Biradical **7**•• differs from **5**•• by the extended π-conjugation in the bridge, due to the replacement of the ester linkages by alkin groups. Therefore an exchange coupling J through bond
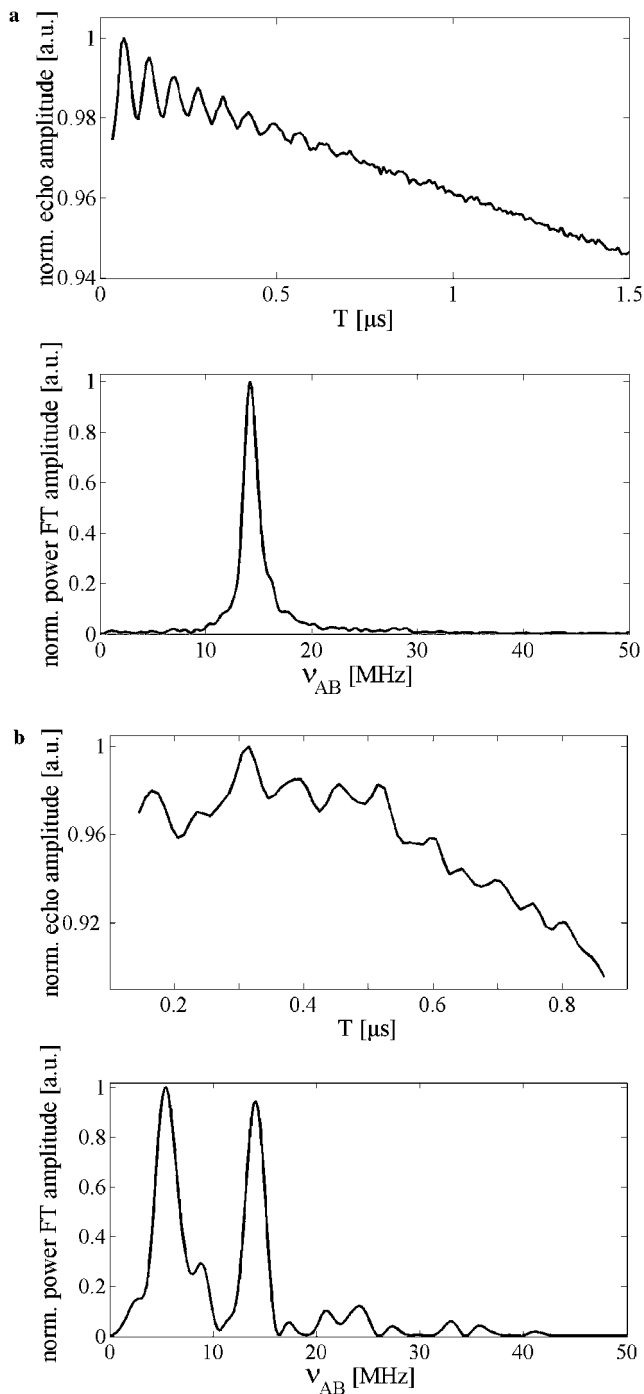
FIG. 6. Three-pulse PELDOR spectra of **5**•• in d_8-toluene (a) at X-band with $\Delta\nu = 80$ MHz, the Fourier-transformed spectrum is shown below, and (b) at S-band with $\Delta\nu = 80$ MHz, the Fourier-transformed spectrum is shown below.
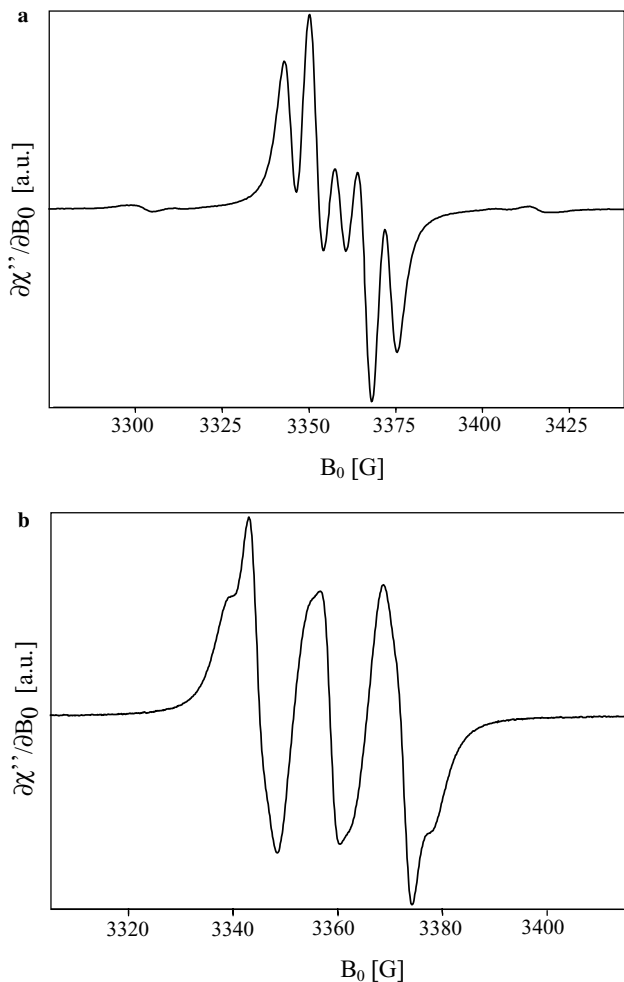
FIG. 7. Continuous wave X-band EPR spectra of (a) $7^{\bullet\bullet}$ and (b) $8^{\bullet\bullet}$ in d_8-toluene at room temperature.

is possible for $7^{\bullet\bullet}$, but suppressed for $5^{\bullet\bullet}$ by the σ-bonds of the ester groups. On the other hand molecular modeling revealed that their r_{AB} are similar with 15.5 Å for $5^{\bullet\bullet}$ and 16.4 Å for $7^{\bullet\bullet}$. The same holds for the couple $6^{\bullet\bullet}$ and $8^{\bullet\bullet}$, here the r_{AB} are 19.7 and 21.0 Å, respectively. The existence of J in $7^{\bullet\bullet}$ and $8^{\bullet\bullet}$ was proven by room temperature cw X-band EPR spectroscopy (Fig. 7). Simulating the spectra yielded values for $|J|$ of 73 and 12 MHz for $7^{\bullet\bullet}$ and $8^{\bullet\bullet}$, respectively. Contrarily, no splitting or line broadening was observable in the room temperature cw spectra of molecules $3^{\bullet\bullet}$–$6^{\bullet\bullet}$, which confirms independently and once more that J is negligible for them. The sign of J cannot be determined by this method.

Biradical $7^{\bullet\bullet}$ exhibits in the PELDOR spectrum no ν_{AB} oscillation or echo decay at S- as well as at X-bands, which is ascribed to the relatively strong exchange coupling of 73 MHz leading to a spin state of the molecule which is rather described by a triplet and a singlet state than by two weakly interacting doublet states needed for PELDOR to be applied successfully. The small distance of 16.4 Å between the two N–O groups is

not the reason for the failure of PELDOR since the even shorter distance of 15.5 Å can be measured in the case of $5^{\bullet\bullet}$. This may point to the possibility of measuring even shorter distances with PELDOR as long as the exchange-coupling J is small enough.

The X-band PELDOR spectra of $8^{\bullet\bullet}$ and their Fourier transformations are shown in Fig. 8. The tensor singularities are
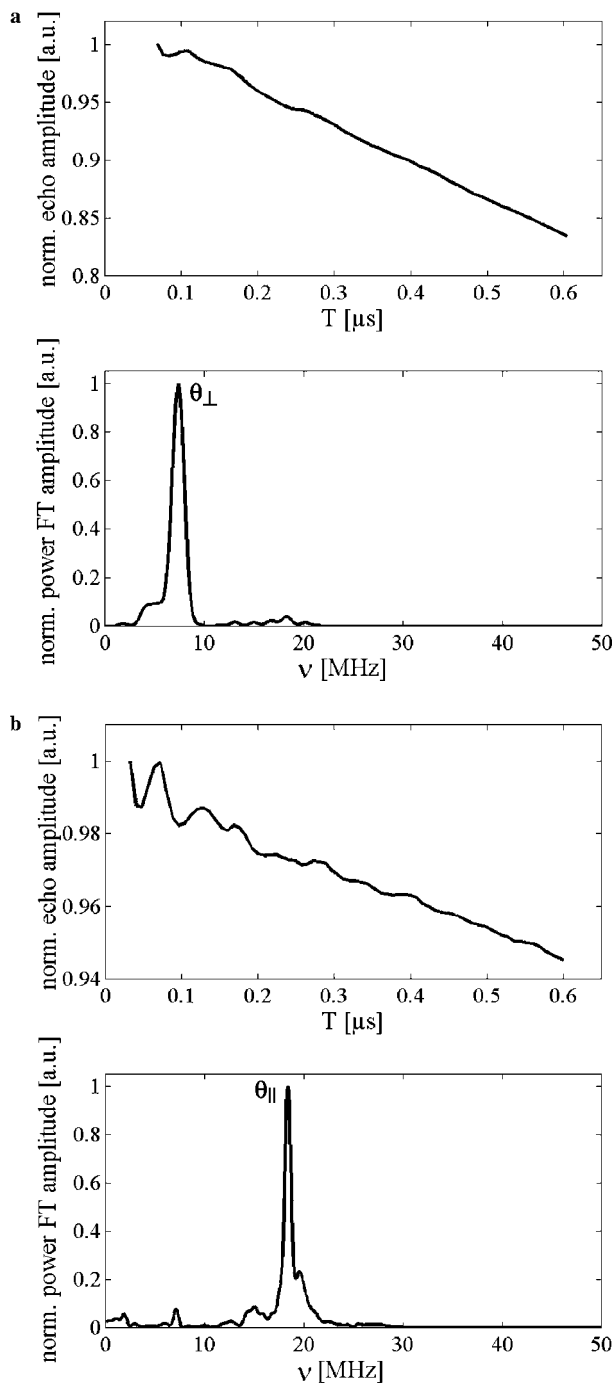
FIG. 8. X-band 3-pulse PELDOR spectra of $8^{\bullet\bullet}$ with (a) $\Delta\nu = 80$ MHz (in d_8-toluene) and (b) $\Delta\nu = 40$ MHz (in h_8-toluene). The Fourier-transformed spectra are shown below the time spectra.

visible at 7.2 MHz for $\Delta\nu = 80$ MHz (Fig. 8a) and at 18.3 MHz for $\Delta\nu = 40$ MHz (Fig. 8b), corresponding to $\theta_\perp$ and $\theta_\parallel$, respectively. As expected in the event of a non-zero J the frequency ν_{AB} at $\theta_\parallel$ is not twice the one at $\theta_\perp$. Since both singularities are detected ν_{Dip} and J can be disentangled from ν_{AB} using Eqs. [6] and [7]. The calculation yields $J = +11$ MHz (antiferromagnetic) and $\nu_{Dip} = 3.7$ MHz. The absolute value of J gathered from the PELDOR measurements fits perfectly the one from the cw EPR measurements. Additionally it reveals the sign and therefore the antiferromagnetic nature of J in $\mathbf{8^{\bullet\bullet}}$ in agreement with the knowledge that a *para*-substituted benzene facilitates usually an antiferromagnetic and not a ferromagnetic spin–spin coupling (*30*). From ν_{Dip} an r_{AB} of 24 Å is calculated which is longer than the computed one of 21 Å. The reason for that may be the failure of the point dipole approximation used for the derivation of Eqs. [4] and [5] owing to the influence of the exchange coupling J. It is interesting that J also seems to have an influence on the orientation selection, since the peak for $\theta_\parallel$ is stronger than the one for $\theta_\perp$ at $\Delta\nu = 40$ MHz, in contrast to the orientation selection for the molecules with $J \cong 0$.

CONCLUSIONS

We introduced a technical setup for PELDOR working at S-band frequencies and tested it successfully on two bisnitroxides known in the literature. Its performance is compared with a setup at X-band frequencies. Being able to perform PELDOR in two frequency bands makes it possible to identify hyperfine coupling contributions. A disadvantage for PELDOR at S-band is the ESEEM behavior at this low field, which allows only the use of a few τ values for the detection sequence. The orientation selectivity is not significantly different at S-band compared to X-band, attributed to the small g anisotropy and the dominating $A_{ZZ}(^{14}N)$ hyperfine-coupling contribution of the nitroxides used here. This may be different for PELDOR measurements on systems containing metal ions, e.g., molybdenum or copper.

Furthermore we synthesized the biradicals $\mathbf{5^{\bullet\bullet}}$–$\mathbf{8^{\bullet\bullet}}$. For molecules $\mathbf{5^{\bullet\bullet}}$ and $\mathbf{6^{\bullet\bullet}}$ the experimental r_{AB} match the theoretical ones very well. For biradical $\mathbf{7^{\bullet\bullet}}$ with an r_{AB} of 16.4 Å and a J of 73 MHz no PELDOR oscillation was observable, whereas the PELDOR oscillation was recovered for $\mathbf{5^{\bullet\bullet}}$ with an even shorter r_{AB} of 15.4 Å but with $J \cong 0$ MHz. For bisnitroxide $\mathbf{8^{\bullet\bullet}}$ it was possible to disentangle ν_{Dip} from J and to ascertain the magnitude and sign of J to $+11$ MHz (antiferromagnetic spin–spin coupling). However, the experimental r_{AB} of 24 Å came out longer than the theoretically predicted one of 21 Å. This may indicate that the lower distance limit for PELDOR is dictated by the magnitude of J. Currently we are using PELDOR for structure determination of doubly spin-labeled RNA.

REFERENCES

1. S. Schlick (Ed.), "Ionomers: Characterization, Theory, and Applications," CRC Press, New York (1996).

2. A. Messerschmidt, R. Huber, T. Poulos, and K. Wieghardt (Eds.), "Handbook of Metalloproteins," Wiley, New York (2001).

3. R. F. Gesteland, T. R. Cech, and J. F. Atkins (Eds.), "The RNA World," Cold Spring Harbor Laboratory Press, Cold Spring Harbor, New York (1999).

4. N. Ban, P. Nissen, J. Hansen, P. B. Moore, and T. A. Steitz, The complete atomic structure of the large ribosomal subunit at 2.4 Å resolution, *Science* **289,** 905 (2000).

5. N. G. Walter, K. J. Hampel, K. M. Brown, and J. M. Burke, Tertiary structure formation in the hairpin ribozyme monitored by fluorescence resonance energy transfer, *EMBO* **17,** 2378 (1998).

6. C. Richter, B. Reif, C. Griesinger, and H. Schwalbe, NMR spectroscopic determination of angles α and ζ in RNA from CH-dipolar coupling, P-CSA cross-correlated relaxation, *J. Am. Chem. Soc.* **122,** 12728 (2000).

7. T. F. Prisner, M. Rohrer, and F. MacMillan, Pulsed EPR spectroscopy: Biological applications, *Annu. Rev. Phys. Chem.* **52,** 279 (2001).

8. L. J. Berliner (Ed.), "Biological Magnetic Resonance," Vol. 14, Plenum, New York (1998).

9. E. J. Hustedt and A. H. Beth, Structural information from CW-EPR spectra of dipolar coupled nitroxide spin labels, *in* "Biological Magnetic Resonance" (L. J. Berliner, S. S. Eaton, and G. R. Eaton, Eds.), Vol. 19, pp. 155–184, Kluwer Academic/Plenum, New York (2000).

10. S. S. Eaton and G. R. Eaton, Distance measurements by CW and pulsed EPR, *in* "Biological Magnetic Resonance" (L. J. Berliner, S. S. Eaton, and G. R. Eaton, Eds.), Vol. 19, p. 8, Kluwer Academic/Plenum, New York (2000).

11. (a) A. D. Milov, K. M. Salikhov, and M. D. Shirov, Application of ELDOR in electron-spin echo for paramagnetic center space distributions in solids, *Fiz. Tverd. Tela* **23,** 975 (1981); (b) A. D. Milov, A. B. Ponomarev, and Yu. D. Tsvetkov, Electron electron-double resonance in electron-spin echo model biradical systems and the sensitized photolysis of decalin, *Chem. Phys. Lett.* **110,** 67 (1984).

12. (a) M. Pannier, S. Veit, A. Godt, G. Jeschke, and H. W. Spiess, Dead-time free measurement of dipole-dipole interactions between electron spins, *J. Magn. Reson.* **142,** 331 (2000); (b) R. E. Martin, M. Pannier, F. Diederich, V. Gramlich, M. Hubrich, and H. W. Spiess, Determination of end-to-end distances in a series of TEMPO diradicals of up to 2.8 nm length with a new four-pulse double electron electron resonance experiment, *Angew. Chem. Int. Ed.* **37,** 2834 (1998).

13. G. Jeschke, M. Pannier, A. Godt, and H. W. Spiess, Dipolar spectroscopy and spin alignment in electron paramagnetic resonance, *Chem. Phys. Lett.* **331,** 243 (2000).

14. J. G. Powles and P. Mansfield, *Phys. Lett.* **2,** 58 (1962).

15. V. V. Kurshev, A. M. Raitsimring, and Y. D. Tsvetkov, Selection of the dipolar interaction by the "$2 + 1$" pulse train, *J. Magn. Reson.* **81,** 441 (1989).

16. S. Saxena and J. H. Freed, Double quantum two-dimensional Fourier transform spin resonance: Distance measurements, *Chem. Phys. Lett.* **251,** 102 (1996).

17. A. Raitsimring, R. H. Crepeau, and J. H. Freed, Nuclear modulation effects in "$2 + 1$" electron spin-echo correlation spectroscopy, *J. Chem. Phys.* **102,** 8746 (1995).

18. (a) A. V. Astashkin, J. H. Enemark, V. V. Kozlyuk, J. MacMaster, and A. M. Raitsimring, Pulsed electron-electron double resonance of paramagnetic centers with large g-value separation, *in* "41st Rocky Mountain Conference on Analytical Chemistry," p. 69 (1999); (b) J. H. Enemark, A. Astashkin,

R. Kedia, V. Kozliouk, J. McMaster, A. Pacheco, A. M. Raitsimring, and M. Valek, Pulsed electron–electron double resonance (ELDOR) studies of Mo(V)/Fe(III) centers, *J. Inorg. Biochem.* **74,** 123 (1999).

19. A. D. Milov, A. G. Maryasov, and Y. D. Tsvetkov, Pulsed electron double resonance (PELDOR) and its applications in free-radicals research, *Appl. Magn. Reson.* **15,** 107 (1998).

20. T. Kálai, M. Balog, J. Jekö, and K. Hideg, Synthesis and reactions of a symmetric paramagnetic pyrrolidine diene, *Synthesis* **6,** 973 (1999).

21. A. Godt, C. Franzen, S. Veit, V. Enkelmann, M. Pannier, and G. Jeschke, EPR probes with well-defined, long distances between two or three unpaired electrons, *J. Org. Chem.* **65,** 7575 (2000).

22. S. Grimaldi, F. MacMillan, T. Ostermann, B. Ludwig, H. Michel, and T. F. Prisner, QH ubisemiquinone radical in the bo3-Type ubiquinol oxidase studied by pulsed electron paramagnetic resonance and hyperfine sublevel correlation spectroscopy, *Biochemistry* **40,** 1037 (2001).

23. A. Weber, M. Rohrer, J. T. Törring, and T. F. Prisner, A CW and pulsed S-band spectrometer, *in* "Proceedings of the 29th Congress AMPERE/13th ISMAR" (D. Ziessow, W. Lubitz, and F. Lendzian, Eds.), Vol. 2, p. 1138 (1998).

24. G. Feher, Sensitivity considerations in microwave paramagnetic resonance absorption techniques, *Bell Syst. Tech. J.* **36,** 449 (1957).

25. M. Willer, J. Forrer, J. Keller, S. Van Doorslaer, and A. Schweiger, S-band (2–4 GHz) pulse electron paramagnetic resonance spectrometer: Construction, probe head design, and performance, *Rev. Sci. Instrum.* **71,** 2807 (2000).

26. R. G. Larsen and D. J. Singel, Double electron–electron resonance spin-echo modulation: Spectroscopic measurement of electron spin pair separations in orientationally disordered solids, *J. Chem. Phys.* **98,** 5134 (1993).

27. M. Pannier, V. Schädler, M. Schöps, U. Wiesner, G. Jeschke, and H. W. Spiess, Determination of ion cluster sizes and cluster-to-cluster distances in ionomers by four-pulse double electron electron resonance spectroscopy, *Macromolecules* **33,** 7812 (2000).

28. The broad components of the tensor vanish in the dead time of the 3-pulse experiment. However, they were recovered by applying the 4-pulse PELDOR sequence. Nevertheless, it turned out that it is difficult to obtain a precise frequency for the $\theta_\parallel$ singularity from these spectra.

29. (a) R. B. Clarkson, M. D. Timken, D. R. Brown, H. C. Crookham, and R. L. Belford, Enhancement of nuclear modulation in electron spin echoes at low magnetic fields: S-band ESE spectrometer, *Chem. Phys. Lett.* **163,** 277 (1989). (b) J. H. Hankiewicz, C. Stenland, and L. Kevan, Pulsed S-band electron spin resonance spectrometer, *Rev. Sci. Instrum.* **64,** 2850 (1993).

30. O. Kahn, "Molecular Magnetism," VCH, New York (1993).